

Grain growth in AZ31 alloy after uniaxial compression

S. ABDESSAMEUD, H. AZZEDDINE, B. ALILI, D. BRADAI,

Laboratoire « Physique des Matériaux », Faculty of Physics, University of Sciences and Technology Houari Boumediene (USTHB), BP32, El-Alia Bab Ezzouar, Algiers 16111, Algeria

Received 4 December 2009; accepted 4 February 2010

Abstract: The grain growth morphology, kinetics and texture change after uniaxial compression at 430 °C of an extruded AZ31 alloy were studied. The samples were loaded following two routes insuring two initial textures of the samples with compression direction parallel and normal to the extrusion direction. For both initial textures, a stable grain size is attained upon isothermal annealing and the grain growth kinetics can be described by: $d^n = d_R^n + kt$ with an n value of around 15. The annealing texture with grown grains is a retained hot deformation texture without emerging or strengthening other components. Abnormal grain growth is not observed for annealing time up to 10 000 h at 450 °C.

Key words: AZ31; magnesium alloy; uniaxial compression; annealing; grain growth; texture

1 Introduction

The improvement of the superplasticity (SP) of wrought AZ31 alloys has been the subject of thorough research activities during the last decades. SP can be achieved via grain refinement using thermomechanical processing. However, Mg-based alloys are subjected to grain growth at high temperature, which reduces SP. The prevention or even inhibition of grain growth may be essentially indispensable to attain SP by retaining the critical conditions for superplastic flow in Mg-based alloys[1].

It was reported that static and isochronal annealing of hot deformed magnesium alloy AZ31 resulted in grain coarsening without texture change relative to recrystallization[2–5]. Such normal grain growth took place upon moderate annealing, while abnormal grain growth took place upon severe annealing[4]. Significant texture changes after severe heat treatments in an AZ31 alloy was observed. In particular, grains with a $\{11\bar{2}0\}$ axis perpendicular to the sheet surface tended to grow abnormally at the expense of grains with other orientations [4]. The formation of very large grains or a large scatter of the grain size in a material due to the abnormal grain growth could drastically deteriorate the properties of the material[6].

Isochronal annealing and texture changes of an AZ31 alloy hot deformed by compression at 300 °C were

characterized through SEM/EBSD analysis[5]. The main conclusion drawn by these authors is that the annealing processes in hot deformed magnesium alloys with initial grain structure obtained by continuous dynamic recrystallization (CDRX) is controlled by a process of grain coarsening without the evolution of the preferred orientations produced by continuous static recrystallization (CSRX). However, isothermal and prolonged annealing investigations of grain growth kinetics in hot rolled AZ31 have not been analyzed yet. A systematic study of the morphology and kinetics of normal and abnormal grain growth and the texture evolution in hot deformed and annealed AZ31 alloys is lacking.

Recently, in Aachen group[7–11], a special consideration was confined to the deformed and recrystallized microstructure and texture of extruded AZ31 alloy. This work seeks to gain insight into the type of grain growth, kinetics and the texture evolution in a commercial AZ31 alloy hot deformed by uniaxial compressing for different initial textures and annealed at 450 °C.

2 Experimental

The material used in this study is an extruded commercial AZ31B alloy provided by Otto Fuchs KG (Germany). The chemical composition is Mg-2.92%Al-0.84%Zn-0.33%Mn-0.02%Si-0.004%Fe-0.001%Cu-

0.001%Ni (mass fraction). Cylindrical (d 15 mm×25 mm) specimens were machined from the extruded rod in two different orientations with the compression axis parallel and perpendicular to the extrusion axis (Fig.1). Two types of samples with different starting texture labelled CD0ED and CD90ED were then obtained. 0 and 90 stand for the compression direction (CD) parallel and normal to the extrusion direction (ED), respectively.

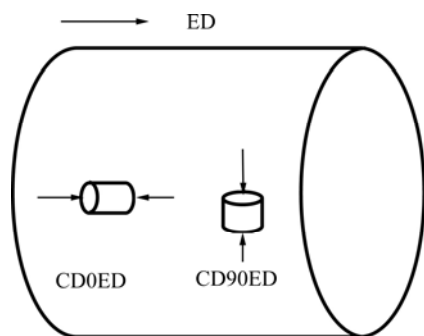


Fig.1 Schematic diagram of sample cutting for uniaxial compression test

Uniaxial compression tests were performed on a ZWICK-1484 electro-mechanical testing machine. The temperature, strain rate and final true strain were fixed to 430 °C, 10^{-4} s^{-1} and 1.4, respectively. The experimental equipment and procedure were described in Refs.[7–11].

The two post deformation specimens show different shape changes and textures after deformation.

The macrotexture was determined in the center plane by measuring incomplete pole figures ($5^\circ \leq \alpha \leq 75^\circ$) in the back reflection mode using CoK_α radiation from an X-ray-texture goniometer. A set of six pole figures ($\{10\bar{1}0\}$, $\{0002\}$, $\{10\bar{1}1\}$, $\{10\bar{1}2\}$, $\{11\bar{2}0\}$ and $\{10\bar{1}3\}$) were measured. The initial and final textures (CD0ED and CD90ED before and after deformation and post deformation annealing) were represented by the recalculated $\{0002\}$ pole figures.

Microstructural examination was performed by optical microscopy. Surface preparation consisted of grinding with progressively finer SiC paper followed by mechanical polishing using diamond solution with particle sizes ranging from 1 to 3 μm . Revealing of the grain structure was achieved by subsequent etching in a solution of acetic picral at room temperature. Average grain sizes were calculated from the optical micrographs by linear intercept method.

3 Results and discussion

Microstructure and texture evolution of the as extruded- and post deformed-alloys were described and analyzed in details in Refs.[10, 12], and the main results are summarized below.

3.1 Microstructure and texture of as extruded alloy

Figs.2(a)-(b) show the microstructures of the as extruded alloy with starting texture labelled CD0ED and CD90ED, respectively. Fig.2(a) is characterized by a

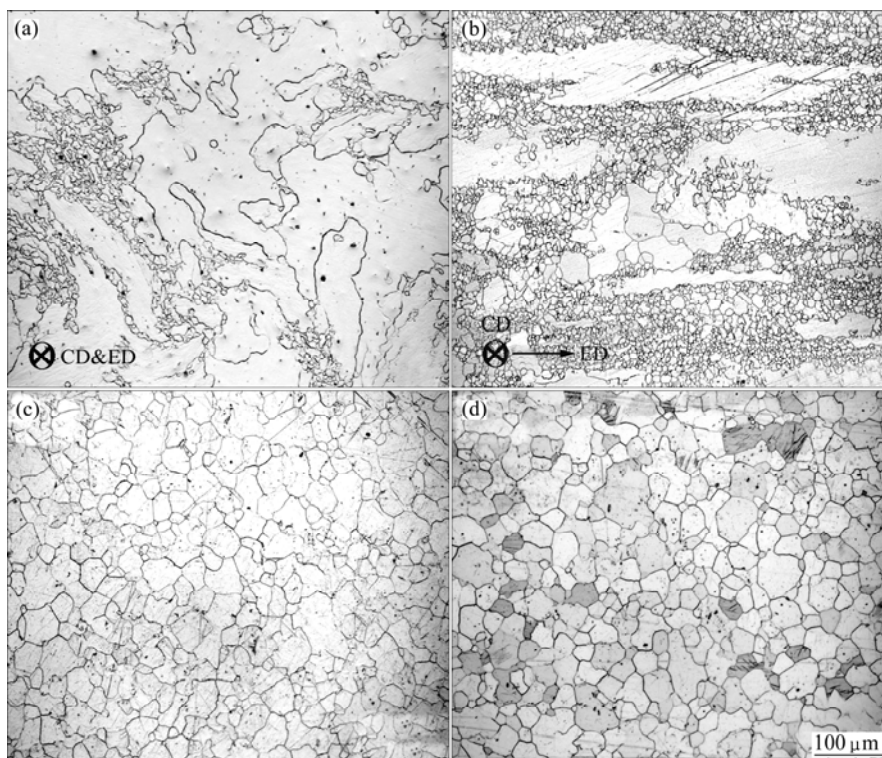


Fig.2 Optical micrographs of AZ 31 alloy: (a) As extruded CD0ED; (b) As-extruded CD90ED; (c) As deformed CD0ED; (d) As-deformed CD90ED

typical hot extrusion microstructure with clusters of recrystallized grains surrounded by large grains. Fig.2(b) shows the starting microstructure of CD90ED specimen (extruded condition) which comprises long bands parallel to the extrusion direction in addition to small recrystallized grains present between those bands. The mean length of the bands was 1–2 mm and the width ranged between 100 and 200 μm . The loading direction was normal to these bands.

The corresponding texture of both samples is presented in Fig.3 by the recalculated $\{0002\}$ pole figures. The extruded material shows a typical extrusion fibre

texture. The basal planes are parallel to the compression direction in the CD0ED specimen and perpendicular to it in the CD90ED specimen. In the extruded samples, the basal planes are parallel to the extrusion direction while the c -axis is perpendicular to the extrusion direction and lying radially among the circles of the cylindrical extrusion geometry.

3.2 Microstructure and texture of as deformed alloy

The uniaxial compression test resulted in shape and texture changes. Fig.4 shows that the round shape geometry of the sample is retained upon the deformation

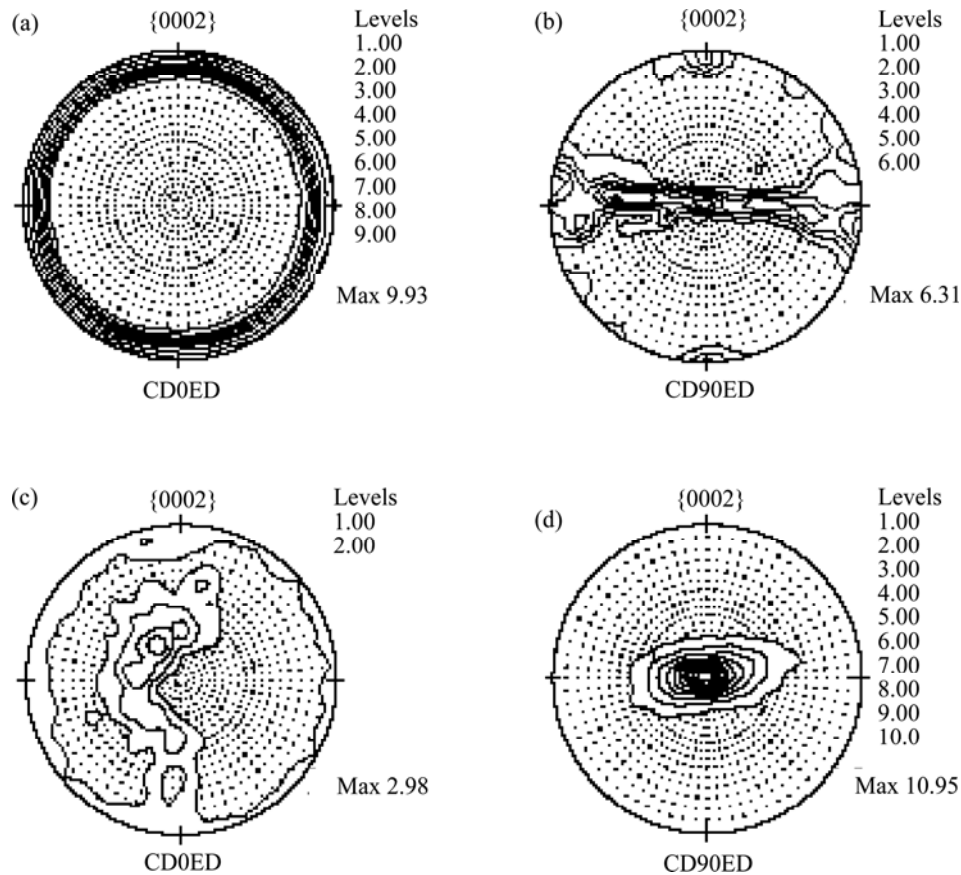


Fig. 3 Texture of the AZ31 alloy: (a) Extrusion CD0ED; (b) Extruded CD90ED and 430°C; (c) Deformed CD0ED; (d) Deformed CD90ED

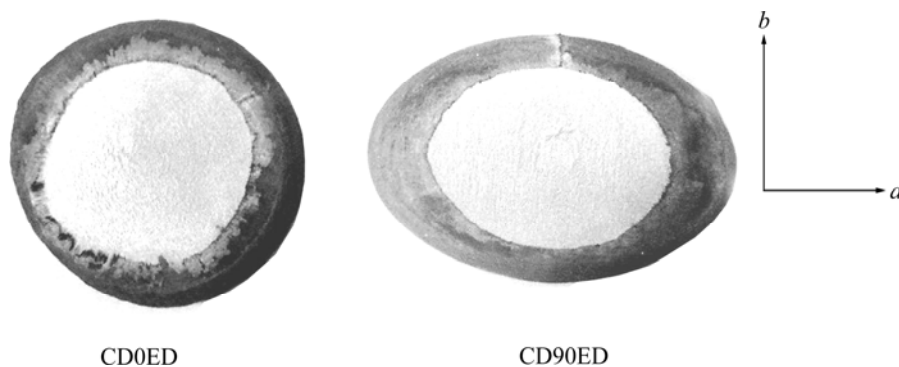


Fig.4 Photos of AZ31 samples deformed by uniaxial compression at 430°C and annealed at 450°C, true strain and strain rate of 140 % and 10^{-4}s^{-1} , respectively

of the CD0ED sample (basal planes parallel to the compression direction before deformation). This is an evidence of an isotropic plastic flow of the material in its all radial directions. The shape of the CD90ED sample changes to elliptical proofing that more flows exist in the “*a*” direction than in the “*b*” direction. The loading direction is normal to the front page. Different initial textures result in different macro morphology due to a competing mechanism of slip and twinning. The activation of crystallographic slip on basal and non-basal planes as well as the activation of twinning is easier for some initial orientations than for others[13].

Figs.2(c) and (d) show the microstructures of the as deformed alloy with the starting texture labelled CD0ED and CD90ED, respectively. Microstructures of all samples show fully recrystallized equiaxed imputable to discontinuous recrystallization (DRX) that was established to happen during uniaxial compression even at lower temperature[11].

Fig.3(c) shows that the CD0ED samples have a weak final texture after uniaxial compression deformation that contrasts totally the initial texture. The evolution of the texture after uniaxial compression deformation showed strong dependence on the temperature and the strain rate[10, 14]. As assumed by AL-SAMMAN et al[10], such weakening seemed due to the activation at 430 °C which is a relatively high deformation temperature of the three possible slip mechanisms, that are $\langle a \rangle$ basal slip, prismatic $\langle a \rangle$ slip and $\langle c+a \rangle$ pyramidal slip. Fig.3(d) shows a basal texture with a strong single peak for the CD90ED sample. This texture was stable even after full annealing at high deformation temperature[15].

In contrast to CD0ED, the texture is sharpened, indicating that basal slip is the preferred deformation mechanism for this sample at temperatures ranging from 200 to 400 °C as pointed out in Ref.[10].

3.3 Microstructure, kinetics and texture of grain growth

Figs.5(a)–(f) present the microstructure evolution of the CD0ED and CD90ED samples aging at 450 °C. Micrographs are obtained along the plane perpendicular to the compression direction in the center of the samples. Microstructures of all samples show fully recrystallized equiaxed grains at all ageing conditions. There is a relatively broad range of grain sizes and shapes of samples annealing for 1.5 h which becomes narrower for longer annealing time. The average grain size increased with increasing annealing time. The changes in the mean grain size of AZ31 alloys with the two initial textures are shown in Fig.6. The grains coarsen upon annealing in a continuous process is called normal grain growth. After an initial transient period of growth, the microstructure

reaches a quasi-stationary state. The difference of the mean grain size value of the two samples does not exceed 10% of the initial grain size. The initial texture prior to deformation shows negligible effect on the final grain size of the samples.

In Ref.[16], the kinetics of normal grain growth under isothermal annealing conditions is expressed as:

$$d^n = d_R^n + kt \quad (1)$$

where d_R is the recrystallized grain size, k is a temperature-dependent constant and n is usually referred to the grain growth exponent. The values of the grain growth exponent n deduced from Fig.6 are equal to 14 and 15 for the CD0ED and CD90ED samples, respectively. These values are much higher than the tabulated ones for different metals and intermetallic systems[17–19], implying that grain growth kinetics in AZ31 alloy is rather complex.

In previous works, grain growth of hot rolled TRC AZ31 alloy with different reductions and annealing temperatures was investigated at 400 and 450 °C[20]. Annealing of the hot rolled samples resulted in normal grain growth with quite similar range of grain size values. A stable grain size was also attained and the grain growth kinetics was described by Eq.(1) with n ranging from 5 to 8. In previous works, the basal initial texture was retained after annealing with total absence of another texture.

Previous microstructural and texture analysis did not reveal any appearance of abnormal grain growth or secondary recrystallization as observed in similar AZ31 and AZ61 alloys[4–5]. Even if the alloys studied are similar, the thermomechanical routes producing the initial state for the grain growth annealing are totally different. Grain growth of annealed alloy cut directly from the received material in as extruded state were analyzed[4–5]. A net through thickness texture gradient existed in their material. In the outer surfaces, basal and $\{11\bar{2}0\}$ prismatic components predominated; in the mid-layer, basal, $\{10\bar{1}0\}$ and $\{11\bar{2}0\}$ prismatic components predominated. A pure predominantly basal texture was observed neither in the outer surface nor in the mid-layer. Upon annealing, in the mid-layer, grains with $\{11\bar{2}0\}$ prismatic planes parallel to the sheet plane grew normally at the expense of randomly oriented grains; while in the outer surface, abnormal growth of grains with $\{11\bar{2}0\}$ prismatic planes occurred.

In the present study, the samples were cut from the extruded material and deformed by hot uniaxial compression. The extruded material shows a typical extrusion fibre texture with $\{0002\}$ basal planes lying parallel to the extrusion axis (i.e. fibre axis perpendicular

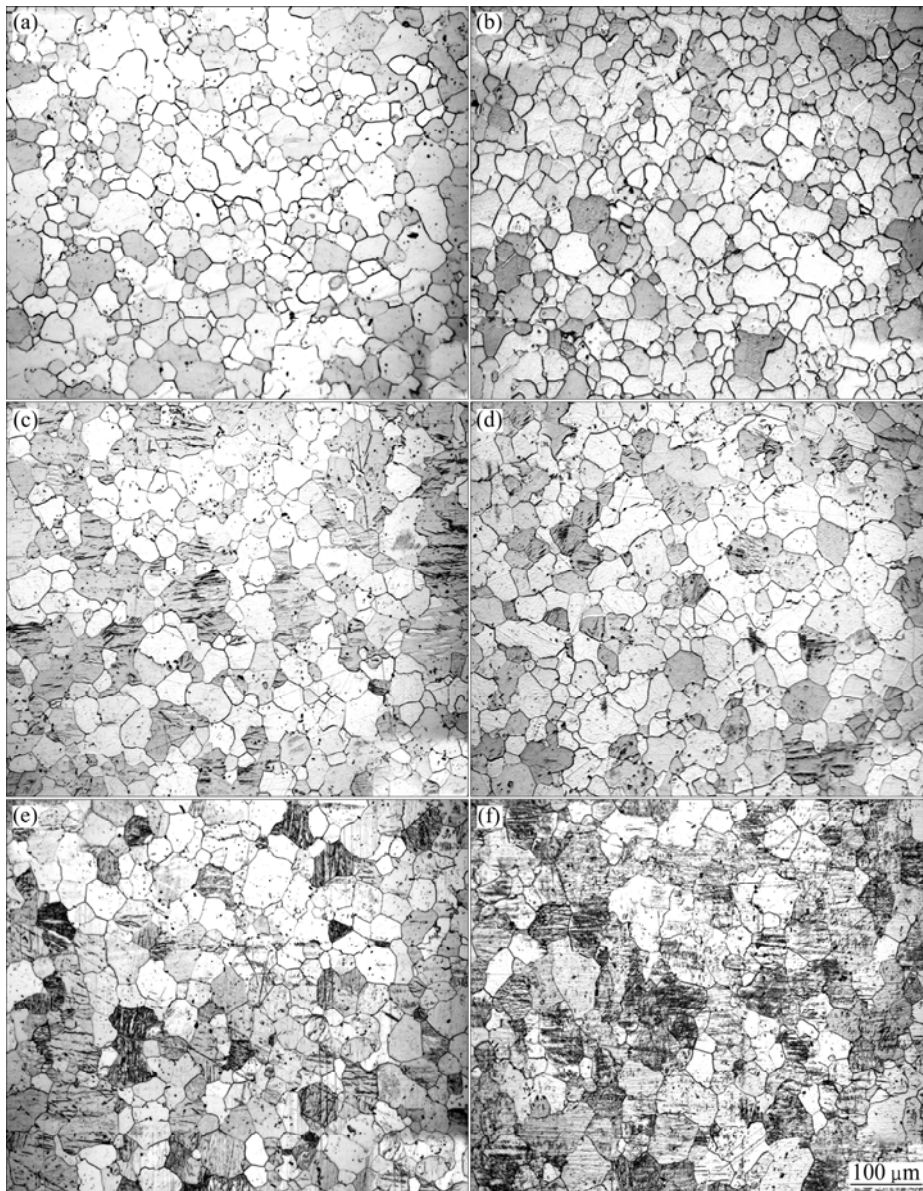


Fig.5 Microstructures of uniaxially compressed AZ31 alloy with initial texture CD0ED annealing for 1.5 h (a), 24 h (c), 7 d (e), CD90ED for 1.5 h (b), 24h (d) and 7 d (f)

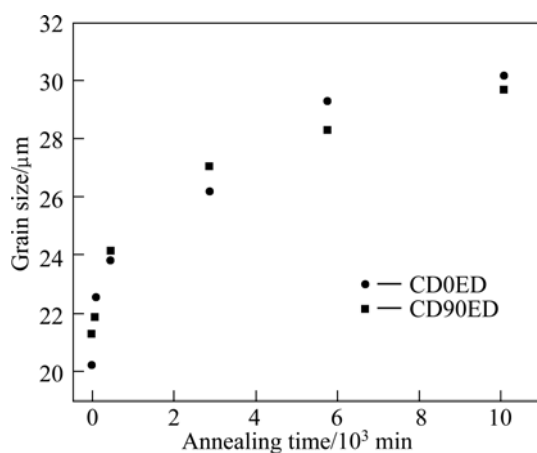


Fig.6 Grain growth kinetics of AZ31 alloy deformed by uniaxial compression at 430 °C and annealed at 450 °C

to the c -axis) as shown in Fig.3. Upon annealing both samples, the texture does not change deeply contrarily to the observations in Refs.[4–5], and as evidenced in Figs.7(a)-(f) and accompanying pole figures (not presented here), there was no trace of the development of the $\{11\bar{2}0\}$ prismatic component or others. We noted a decrease of intensity of the basal poles for the CD90ED samples.

Many metals and alloys with intermetallic particles (with volume fraction between 0.01 and 0.1) can develop the abnormal grain growth but precise conditions of its occurrence or inhibition are still unclear[16, 21]. The six factors that influence the occurrence of abnormal grain growth were discussed, from an initially uniform grain size distribution in materials containing unstable and

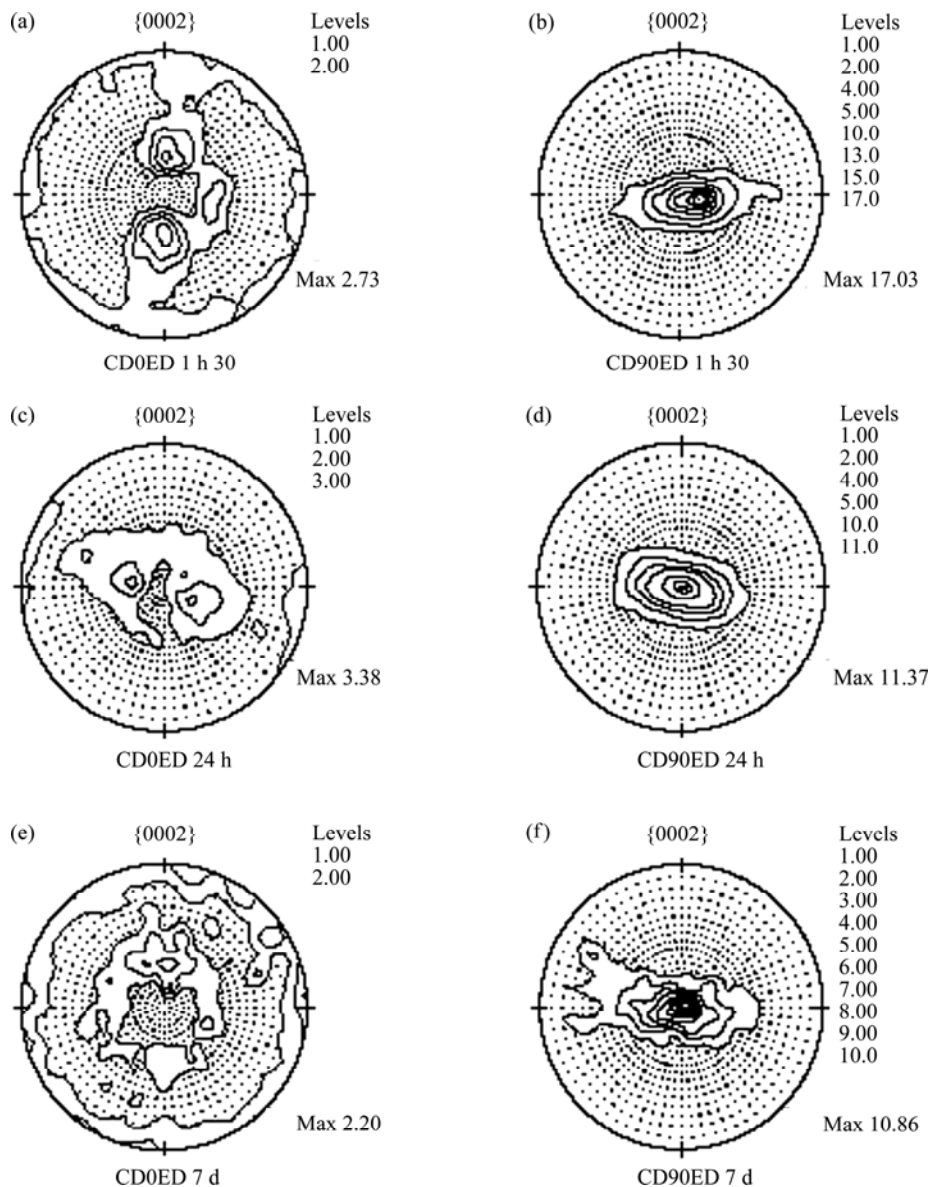


Fig.7 Evolution of grain growth texture at 450°C versus annealing time of AZ31 alloy after uniaxial compression at 430°C with initial texture CD0ED for 1.5 h (a), 24 h (c) and 7 d (e) and CD90ED for 1.5 h (b), 24 h (d) and 7 d (f)

stable particles[22–23]. Among the factors, three are difficult to estimate directly, they are 1) the presence of grains that are able to grow abnormally, 2) the rate of decrease in pinning force and 3) grain boundary energy per unit. In the present study, the abnormal grain growth may be restrained due to 4) the mobility in AZ31 alloys with such Al and Zn solute content and particle dispersion. Potential reasons may be a higher degree of segregation and lower solubility, i.e. higher solute concentration in the boundary, which would increase the solute drag and Zener drag, and thus impede the effective mobility of the boundary. Among the intermetallic particle phases that exist in the AZ31 alloys are the unstable $Mg_{17}Al_{12}$, stable AlMn, FeMn and Mg_2Si [24–25]. The former may be potentially

responsible for Zener drag.

5) The critical radius (approximately identical to the mean grain radius). The smaller the critical radius is, the smaller the relative decrease is in pinning force, which is necessary for abnormal grain growth. Very fine grains pinned by very fine particles (may significantly increase the susceptibility to abnormal grain growth). This is far from the case here that d is 20–30 μm and the particle size of the stable intermetallic phases d_p present in Mg-Al based alloys is found to be 1 μm [26].

6) The distribution width ($n = R_{max}/R_c$, where R_{max} is the maximum radius of grains and R_c is the critical radius) and the broader distributions will be less susceptible to abnormal grain growth. Fig.8 presents the histograms of grain size and a relatively broad lognormal

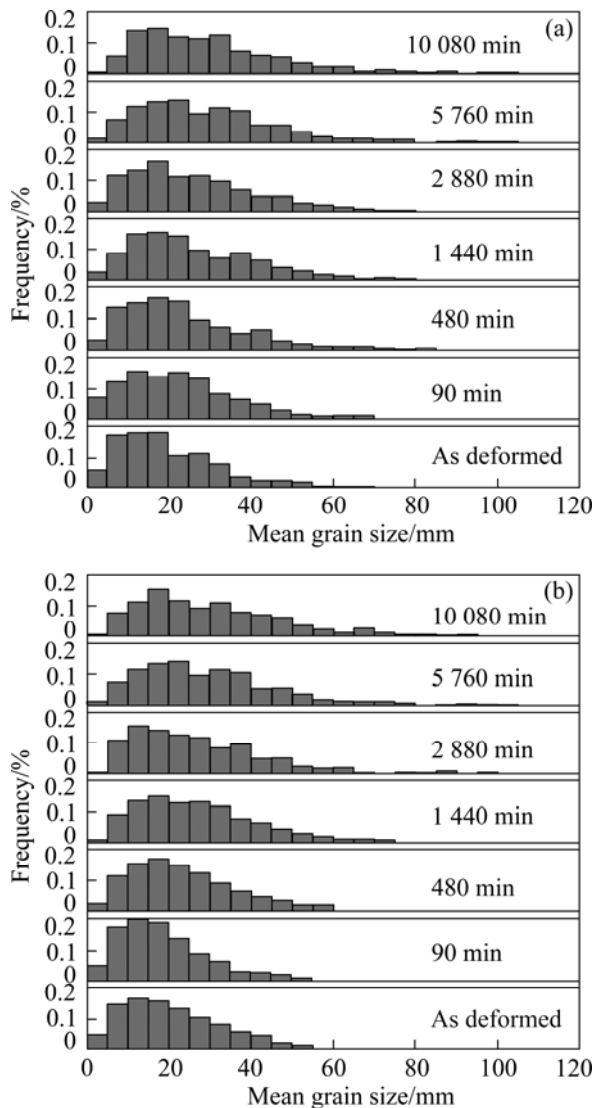


Fig.8 Mean grain size of AZ31 alloy deformed by uniaxial compression at 430 °C and annealed at 450 °C for different time: (a) CD0ED; (b) CD90ED

distribution with standard deviation ranging from 12 to 18 μm for a mean grain size ranging from 20 to 30 μm and the minimal and maximal value of 2 and 120 μm , respectively are evidenced. Such features may be the possible causes of the inhibition of the abnormal grain growth in AZ31 alloy hot deformed by uniaxial compression at 450 °C.

4 Conclusions

1) The grain growth of hot deformed and annealed AZ31 alloy was investigated at 450 °C for two initial textures. Uniaxial compression of the extruded alloy leads to a weak and a strong basal texture for initial samples with compression direction parallel and normal

to the extrusion direction, respectively.

2) Annealing of both the hot deformed samples produces normal grain growth. A stable grain size is attained and the grain growth kinetics is obtained.

3) The annealing texture following grain growth is a retained hot deformation texture without emerging or strengthening of other components. Abnormal grain growth is not observed for annealing time up to 10 000 h at 450 °C.

Acknowledgement

One of the authors S. ABDESSAMEVD wishes to thank Prof. G. GÖTTSTEIN and Dr T. AL-SAMMAN from the Institut für Metallkunde und Metallphysik, RWTH Aachen, for their assistance and help during her scientific stays.

References

- [1] BUSSIBA A, BEN ARTZY A, SHTECHMAN A, IFERGAN S, KUPIEC M. Grain refinement of AZ31 and ZK60 Mg alloys—Towards super plasticity studies [J]. *Mater Sci Eng A*, 2001, 302: 56–62.
- [2] WAGNER F, BOZZOLO N, VAN LANDUYT O, GROSSDIER T. Evolution of recrystallisation texture and microstructure in low alloyed titanium sheets [J]. *Acta Mater*, 2002, 50 (5): 1245–1259.
- [3] PÉREZ-PRADO M T, RUANO O A. Texture evolution during annealing of magnesium AZ31 alloy [J]. *Scripta Mater*, 2002, 46 (2): 49–155.
- [4] PÉREZ-PRADO M T, RUANO O A. Texture evolution during grain growth in annealed Mg AZ61 alloy [J]. *Sripta Mater*, 2003, 48 (1): 59–64.
- [5] YANG X Y, MIURA H, SAKAI T. Recrystallization behaviour of fine-grained magnesium alloy after hot deformation [J]. *Transactions of Nonferrous Metals Society of China*, 2007, 17(6): 1139–1142.
- [6] STRAUMAL B B, GUST W, SURSAEVA V G, SEMENOV V N, SHVINDLERMAN L S. Normal and abnormal grain growth in tungsten polycrystals [J]. *Materials Science Forum*, 1999, 294/296: 533–536.
- [7] GOTTSTEIN G, AL-SAMMAN T. Texture development in pure Mg and Mg alloy AZ31 [J]. *Materials Science Forum*, 2005, 495/497: 623–632.
- [8] GOTTSTEIN G, AL-SAMMAN T. The influence of strain path on texture evolution in magnesium alloy AZ31 [C]//KAINER K U. *Magnesium: Proceedings of the 7th international Conference on Magnesium Alloys and Their Applications*. Dresden, Germany: 2006, 553–559.
- [9] AL-SAMMAN T, GOTTSTEIN G. Deformation conditions and stability of the basal texture in magnesium [J]. *Materials Science Forum*, 2007, 439/543: 3401–3406.
- [10] AL-SAMMAN T, AHMAD B, GOTTSTEIN G. Uniaxial and plane strain compression behaviour of magnesium alloy AZ31: A comparative study [J]. *Materials Science Forum*, 2007, 550: 229–234.
- [11] AL-SAMMAN T. Comparative study of the deformation behavior of hexagonal magnesium-lithium alloys and a conventional magnesium AZ31 alloy [J]. *Acta Mater*, 2009, 57 (7): 2229–2242.

- [12] YANG X Y, MIURA H, SAKAI T. Dynamic recrystallization and texture development during hot deformation of magnesium alloy AZ31 [J]. Transactions of Nonferrous Metals Society of China, 2009, 19(1): 55–60.
- [13] Al-SAMMAN T. Magnesium – The role of crystallographic texture, deformation conditions and alloying elements on formability [D]. Aachen: RWTH University, 2008: 163–164.
- [14] SHI Ti, YU Kun, LI Wen-xian, WANG Ri-chu, WANG Xiao-yan, CAI Zhi-yong. Hot-compression constitutive relation of as-cast AZ31 magnesium alloy [J]. Transactions of Nonferrous Metals Society of China, 2007, 17(S1): s336–s341.
- [15] YANG X Y, SUN Z, XING J, MIURA H, SAKAI T. Grain size and texture changes of magnesium alloy AZ31 during multi-directional forging [J]. Transactions of Nonferrous Metals Society of China, 2008, 18(S1): s200–s204.
- [16] HUMPHREYS F J, HATHERLY M. Recrystallization and related annealing phenomena [M]. Oxford, UK: Pergamon, 1995: 369–384.
- [17] KAWANISHI S, ISONISHI K, OKAZAKI K. Grain growth and its kinetics of nanophase niobium aluminide produced by mechanical alloying [J]. Mater Trans JIM, 1993, 34 (1): 49–53.
- [18] ZHOU L Z, GUO J T. Grain growth and kinetics for nanocrystalline NiAl [J]. Scripta Materialia, 1999, 40(2): 139–144.
- [19] PORTER D A, EASTERLING K E. Phase transformations in metals and alloys [M]. London: Chapman and Hill, 1991: 350.
- [20] ABDESSAMEUD S, BRADAI D. Microstructure and texture evolution in hot rolled and annealed magnesium alloy TRC AZ31 [J]. Canadian Metallurgical Quarterly, 2009, 48 (4): 433–442.
- [21] DUNN C G, WALTER J L. Recrystallization, grain growth and textures [M]. Ohio: ASM, 1966: 461.
- [22] RIOS P R. Abnormal grain growth development from uniform grain size distributions [J]. Acta Mater, 1997, 45 (4): 1785–1789.
- [23] RIOS P R. Abnormal grain growth development from uniform grain size distributions in the presence of stable particles[J]. Scripta Materialia, 1998, 39(12): 1725–1730.
- [24] MATUCHA K H. Materials science and technology: A comprehensive treatment [M]//CAHN R W, HAASEN P, KRAMER E J. Volume 8: Structure and properties of nonferrous alloys. Weinheim, 1996.
- [25] CATON P D. Magnesium – An old material with new applications [J]. Materials and Design, 1991, 12 (6): 309–316.
- [26] DULY D. Etude de la précipitation discontinue dans les alliages Mg-Al [D]. Enseeg, Grenoble: 1992: 279–286. (in French)

(Edited by FANG Jing-hua)